

Decellularized Cartilage-Derived Matrix as Substrate for Endochondral Bone Regeneration

Debby Gawlitta, PhD,^{1,*} Kim E.M. Benders, MD,^{1,*} Jetze Visser, MD,¹ Anja S. van der Sar,²
Diederik H.R. Kempen, MD, PhD,¹ Lars F.H. Theyse, PhD, DVM, ECVS,³
Jos Malda, PhD,^{1,4} and Wouter J.A. Dhert, MD, PhD^{1,5}

Following an endochondral approach to bone regeneration, multipotent stromal cells (MSCs) can be cultured on a scaffold to create a cartilaginous callus that is subsequently remodeled into bone. An attractive scaffold material for cartilage regeneration that has recently regained attention is decellularized cartilage-derived matrix (CDM). Since this material has shown potential for cartilage regeneration, we hypothesized that CDM could be a potent material for endochondral bone regeneration. In addition, since decellularized matrices are known to harbor bioactive cues for tissue formation, we evaluated the need for seeded MSCs in CDM scaffolds. In this study, ectopic bone formation in rats was evaluated for CDM scaffolds seeded with human MSCs and compared with unseeded controls. The MSC-seeded samples were preconditioned in chondrogenic medium for 37 days. After 8 weeks of subcutaneous implantation, the extent of mineralization was significantly higher in the MSC-seeded constructs versus unseeded controls. The mineralized areas corresponded to bone formation with bone marrow cavities. In addition, rat-specific bone formation was confirmed by collagen type I immunohistochemistry. Finally, fluorochrome incorporation at 3 and 6 weeks revealed that the bone formation had an inwardly directed progression. Taken together, our results show that decellularized CDM is a promising biomaterial for endochondral bone regeneration when combined with MSCs at ectopic locations. Modification of current decellularization protocols may lead to enhanced functionality of CDM scaffolds, potentially offering the prospect of generation of cell-free off-the-shelf bone regenerative substitutes.

Introduction

PREVIOUSLY, BONE REGENERATION strategies have predominantly relied on biomimicry of the intramembranous pathway of bone formation. However, this approach has not yet resulted in a new treatment modality for the repair of large bone defects in clinical practice. In recent years, following the concept of developmental engineering,¹ the attention has shifted toward exploration of the feasibility of bone regeneration following an alternative method: the endochondral approach.^{1–5} In the endochondral approach, bone formation starts from a cartilaginous template.⁶ Cells residing in this template undergo terminal chondrogenic differentiation. During the hypertrophic stage of differentiation, these cells initiate the mineralization of the cartilaginous matrix that is surrounding them. Before cell death, angiogenic and chemotactic factors are excreted that can attract cells to

remodel the mineralized cartilage into bone. As a consequence, blood vessels, osteoblasts, and osteoclasts invade the template and replace it with bone tissue.⁶

Multipotent stromal cells (MSCs) are ideal candidate cells for bone regeneration through the endochondral route, as they have the capacity for hypertrophic differentiation under currently applied chondrogenic culture conditions.^{5,7,8} The endochondral approach to bone tissue engineering has proved its feasibility for MSC-containing constructs at ectopic locations in rodents.^{1–5,9,10} In general, MSCs were chondrogenically stimulated *in vitro* and after subcutaneous implantation, the formation of bone tissue was observed. The formed bone was mineralized and contained bone marrow cavities with hematopoietic cells.

Despite its great promise, several challenges remain in the creation of grafts following this approach. A major obstacle is increasing construct size. Endochondral bone formation

¹Department of Orthopedics, University Medical Center Utrecht, Utrecht, The Netherlands.

²Central Laboratory Animal Institute, Utrecht, The Netherlands.

Departments of ³Clinical Sciences of Companion Animals and ⁴Equine Sciences, Faculty of Veterinary Medicine, Utrecht University, Utrecht, The Netherlands.

⁵Faculty of Veterinary Medicine, Utrecht University, Utrecht, The Netherlands.

*These authors contributed equally.

in vivo is either achieved in small pellet cultures^{1,3,5} or restricted to the periphery of larger constructs.² Choosing a scaffold material that can further stimulate and/or accelerate the endochondral process could address this limitation. Since endochondral bone formation is based on the formation of bone from a cartilaginous template, it may be desirable from a developmental engineering standpoint¹ to increase the construct size by increasing the cartilage volume. So, instead of relying on the creation of a cartilaginous matrix by the MSCs only, a logical step would be to add cartilaginous matrix as a scaffold material.

The use of cartilage as a substitute for bone tissue has been vastly explored in the 1950s–1980s of the previous century.^{11–14} It has been shown that autologous or isogenic cartilage transplantation in rats induced bone formation.^{12,14} This effect was affected by donor age and predominantly observed for tissue obtained from young donor animals.^{12,13} Another important prerequisite for *in vivo* bone formation was the presence of viable cartilage cells.^{12,13} In addition, despite its potential in auto and isotransplantation, ossification of the cartilage matrix was never seen in xenotransplantation.¹² This property would render clinical application of decellularized xenogenic cartilage-derived matrix (CDM) limited as a biomaterial for endochondral bone regeneration.

To summarize, recently, the use of decellularized CDM has gained attention and its potential for cartilage regeneration was recognized.^{15–19} Moreover, preliminary *in vivo* studies indicated that a CDM scaffold could be effective in regenerating bone and cartilage in an osteochondral defect

model.¹⁵ In this previous study, the CDM scaffold was cell free, and it remains unknown whether preseeding of the construct with MSCs is a prerequisite for endochondral bone regeneration.

To address the latter, here, we investigated the feasibility of decellularized CDM xenografts as a scaffold material for ectopic endochondral bone regeneration. Our main question was whether the unseeded scaffolds could attract host cells and induce endochondral bone regeneration. This would offer the prospect of generating off-the-shelf bone constructs consisting of CDM only. The performance of the unseeded CDM scaffolds was compared with that of CDM seeded with human MSCs (hMSCs).

Materials and Methods

Experimental design

An overview of the experimental layout is shown in Table 1. The induction of bone tissue formation was evaluated in subcutaneous dorsal pockets of immunocompromised rats. To test the intrinsic osteoinductivity of the CDM scaffold material, samples were either preconditioned with hMSCs (MSC seeded) or remained unseeded. hMSCs were chosen with the eventual application in patients in mind. An equine source was chosen to be able to obtain sufficient amounts of cartilage for CDM preparation and in view of potential translation to both human and equine patients. Moreover, equine cartilage closely resembles human cartilage in both histological and biochemical properties.²⁰

TABLE 1. OVERVIEW OF THE EXPERIMENTAL SET-UP, INCLUDING THE TIME FRAME AND NUMBERS OF SAMPLES

Day

-44

-37

0

21

42

56

MSC-seeded CDM scaffolds

MSC seeding and expansion

Chondrogenic differentiation

Unseeded CDM scaffolds

In vivo implantation
(day 21 xylenol orange,
day 42 calcein green)

Analysis	N	Day
Histology paraffin	3 seeded 3 unseeded	0
	1 seeded	22*
	7 seeded 6 unseeded	56
Histology MMA	7 seeded 7 unseeded	56
X-ray	14 seeded 13 unseeded	56

*One animal died before the intended end of the experiment at day 22.

The MSCs were seeded and expanded before chondrogenic differentiation *in vitro*. The samples were implanted for a total of 8 weeks. The number of samples taken for each analysis varied as indicated in the table.

MSC isolation and culture

A bone marrow aspirate was taken from the iliac crest of a 69-year-old male human patient receiving a total hip arthroplasty after his informed consent according to a protocol approved by the local Medical Ethics Committee (University Medical Center Utrecht). The cells were separated on Ficoll-paque, and the mononuclear fraction was then plated for selection on plastic adherence, as previously described.⁸ The cells were passaged at subconfluency and maintained in expansion medium containing minimum essential medium α (Invitrogen), with 10% heat-inactivated fetal bovine serum (BioWhittaker), 0.2 mM L-ascorbic acid 2-phosphate (Sigma), 100 U/mL penicillin with 100 mg/mL streptomycin (PenStrep; Invitrogen), and 1 ng/mL basic fibroblast growth factor (bFGF; R&D Systems). At passage 4, they were harvested for scaffold seeding.

The potential of the MSCs for multilineage differentiation into adipogenic, osteogenic, and chondrogenic cells was confirmed. In addition, FACS analysis was performed for confirmation of the presence of CD73 (BD Pharmagen), CD90 (Biolegend), and CD105 (Abcam) and for the absence of CD31 (Serotec), CD34 (BD Pharmagen), and CD45 (BD Pharmagen). Isotype-matched controls (Life Science) were also analyzed. Characterization is included in Supplementary Fig. S1 (Supplementary Data are available online at www.liebertpub.com/tea).

Scaffold preparation

Equine cartilage from seven donors (age 3–10) was harvested postmortem from the femoral condyles of the stifle joints after obtaining permission of the owners. The joints were stored at -20°C before tissue harvest. The cartilage was removed from the femoral condyles, cut into small pieces with a surgical blade, and immersed in PBS supplemented with 10% PenStrep and 10% fungizone (Life TechnologiesTM). Next, the cartilage was subjected to multiple enzymatic and mechanical treatment steps, as previously described.²¹ The resulting CDM was transferred into cylindrical molds (3.5 mm diameter, 10 mm high) and freeze dried for 24 h. The scaffolds were cross-linked by UV exposure²² overnight and sterilized using ethylene-oxide. Before cell seeding, the scaffolds were cut to measure 5 mm in height and presoaked for 1 h in expansion medium without bFGF.

Scaffold seeding and differentiation

The hMSCs were seeded onto the porous scaffolds in two steps. In total, 700,000 cells were suspended in 50 μL of expansion medium for each scaffold. In the first round, half of the volume was applied along the mantle of the scaffold cylinder. After 1 h, the scaffolds were turned to 180° before pipetting the second half of the suspension onto the scaffolds. On day 7, the medium was changed from expansion to chondrogenic differentiation medium consisting of high-glucose Dulbecco's modified Eagle's medium (Invitrogen) with 1% ITS+ premix (BD Biosciences), 10^{-7} M dexamethasone (Sigma), 0.2 mM L-ascorbic acid 2-phosphate,

PenStrep, and 10 ng/mL TGF β 2 (R&D Systems). The seeded scaffolds were maintained in 24-well plates, while medium was refreshed twice a week until implantation. After 37 days in differentiation medium, three scaffolds were fixed in formalin for histological analysis.

The two groups of scaffolds that were implanted subcutaneously were either cell seeded as described earlier or unseeded. The unseeded scaffolds were not presoaked before implantation.

Implantation in immunocompromised rats

The experiment in rats was approved by the local Ethics Committee for Animal Experimentation and in compliance with the Institutional Guidelines on the Use of Laboratory Animals. The experiment was performed on male, athymic nude rats (Hsd:RH-Foxn1^{tmu}, 11 weeks; Harlan) that were anesthetized with 2.5% isoflurane and air/oxygen. Subcutaneous pockets were created from 7 to 10 mm dorsal incisions, with each to fit one scaffold. Each pocket was created by blunt dissection through the skin incision and filled with one implant. The skin was closed transcutaneously with Vicryl Rapide sutures (Ethicon). Before and after the operation, the animals received 0.05 mg/kg buprenorphin subcutaneously (Temgesic; Schering-Plough/Merck). The rats were housed in pairs at the Central Laboratory Animal Institute of Utrecht University. At week 3 and 6 after implantation, all animals received subcutaneously administered fluorochromes, 100 mg/kg xylenol orange (Sigma), and 10 mg/kg calcein green (Sigma), respectively. These fluorochromes are known to bind free calcium ions before their incorporation in active mineralization processes, thus indicating sites of active bone formation after the moment of injection.^{23,24} At 8 weeks, the rats were euthanized by CO_2/O_2 inhalation and the scaffolds were explanted and fixed in formalin.

X-ray and fluorescence imaging

While in formalin, the explants were imaged in 2D in a Faxitron[®] X-ray system with a dose of 22 kV for 12 seconds, taking along a femur and tibia of the rats as a positive control. Mineralized areas in the samples were clearly delineated, and their brightness was comparable to that of rat bone controls. Using Adobe Photoshop CS5, the total surface area of the mineralized tissue was quantified and the pixel dimensions were converted to mm^2 . To illustrate the total number of samples of the groups that showed mineral content on the X-ray, a ratio was calculated as follows: ratio of positive X-rays = number of samples with mineral content/total number of samples in the group.

In addition, the explants were examined by whole-mount fluorescence microscopy using a triple filter (Olympus) for simultaneous detection of the red and green fluorochromes. After image analysis, the explants were further processed and embedded in paraffin or methyl methacrylate (MMA).

Histology and immunohistochemistry on paraffin sections

Explanted samples ($n=7$ for MSC-seeded CDM, $n=6$ for unseeded CDM) were decalcified in Luthra solution (0.35 M HCl and 2.65 M formic acid in distilled water), before dehydration, embedding in paraffin, and sectioning (5 μm). For identification of cartilage and bone, a triple stain of safranin-O, fast green, and hematoxylin was used.⁸

Besides subcutaneous implants, these rats had also received samples in one critical defect in one of their femora. However, only subcutaneous samples were included in analyses of this study. One rat died at day 22 after implantation during revision surgery of a loosened internal fixator. Samples retrieved from this animal were not decalcified but fixed in formalin and directly embedded in paraffin. On sections from this animal, mineralization could be visualized by von Kossa staining with Mayer's hematoxylin counterstaining, as well as the presence of tartrate-resistant acid phosphatase (TRAP) in osteoclasts. TRAP is secreted by active osteoclasts that resorb mineralized cartilage or bone in order to be remodeled into new bone. For TRAP staining, sections were deparaffinized and rehydrated, before incubation in 0.2 M acetate buffer containing 50 mM L-(+)-tartaric acid (Sigma) at pH 5.0 for 20 min at room temperature. Next, TRAP activity was stained by adding 0.5 mg/mL Naphtol AS-MX phosphate and 1.1 mg/mL Fast red TR salt (both from Sigma) to this solution and incubating at 37°C for 1–4 h. Finally, the sections were counterstained with Mayer's hematoxylin.

Immunohistochemical detection of collagen types I, II, and X was performed after deparaffinization and rehydration of the sections. The reactivity of the collagen type I antibodies was extensively tested on rat, human, and equine tissues. It was found that the mouse anti-human I-8H5 antibody could recognize both human and equine collagen type I, but not collagen from rat origin. On the other hand, the rabbit anti-rat ABT-123 antibody exclusively detected rat collagen type I and not collagen of equine or human origin.

All sections were blocked to prevent nonspecific binding in 5% bovine serum albumin and 0.3% H₂O₂. For collagen type I (human) and type II, antigen retrieval was performed by incubation with 1 mg/mL pronase (Sigma) and 10 mg/mL hyaluronidase (Sigma) for half an hour each. Retrieval of rat collagen type I was performed by boiling the sections for 10 min in 10 mM citrate buffer, pH 6.0. Collagen type X antigen was retrieved by incubation at 37°C in 1 mg/mL pepsin (Sigma) in 0.5 M acetic acid for 2 h and in 10 mg/mL hyaluronidase (Sigma) for half an hour. Next, sections were incubated with the primary antibodies for collagen type I (1:100, monoclonal mouse anti-human, CP17 clone I-8H5, Millipore; and 1:50, polyclonal rabbit anti-rat, ABT123, Millipore), collagen type II (1:100, monoclonal mouse, II-II6B3; DSHB), and collagen type X (1:20; Quartett), at 4°C overnight. Subsequently, collagen type I (human) and type II sections were incubated with GAM-HRP (1:200, P0447; Dako) at room temperature for an hour. Collagen type I (rat) sections were incubated with both goat anti-rabbit biotinylated antibody (1:200, E0432; Dako) and SA-HRP (1:400; Dako) for 1 h at room temperature. Collagen type X sections were incubated with a biotinylated secondary antibody (1:200; GE Healthcare, RPN1001V) for 1 h at room temperature, after which they were incubated with SA-HRP (1:400; Dako) for an hour at room temperature. All collagen types were detected by a 10-min conversion of 3,3'-diaminobenzidine solution (Sigma). Nuclei were counterstained with 50% Mayer's hematoxylin. Isotype control stainings were carried out with a murine IgG1 monoclonal antibody (Dako) at concentrations matching those used for the primary antibodies or by incubation without primary antibody. The stained sections were examined by using a light microscope (Olympus BX51).

To examine the fate of the implanted cells, human mitochondria were stained. After deparaffinization and rehydration of paraffin sections, the antigen was retrieved by cooking the sections in Tris-EDTA (pH 9, 10 mM Tris-HCl, 1 mM EDTA) at 95°C for 30 min. Then, sections were blocked in 3% H₂O₂, washed, and incubated with the primary antibody overnight at 4°C (1:1000, anti-mitochondria; Abcam). The anti-mouse, HRP-labeled Envision+ system (Dako) was used for 30 min before the staining was performed with the DAB+ Substrate Chromogen System (1:100; Dako). Sections were counterstained with hematoxylin before mounting in depex.

Histology and fluorochrome detection on MMA sections

Undecalcified samples ($n=7$ for both groups) were dehydrated and embedded in polymethylmethacrylate, MMA. Sections of 20–30 μ m were generated along the long axis of the cylindrical samples on a saw Microtome system (Leica 4 SP1600). The axial sections were stained with methylene blue and basic fuchsin and evaluated by light microscopy. In addition, sections were made that remained unstained to evaluate the presence of fluorochromes.

Statistics

The raw data of the 2D quantification of mineralized areas in the Faxitron images were expressed as "pixel²." These data were analyzed with an IBM® SPSS® Statistics,

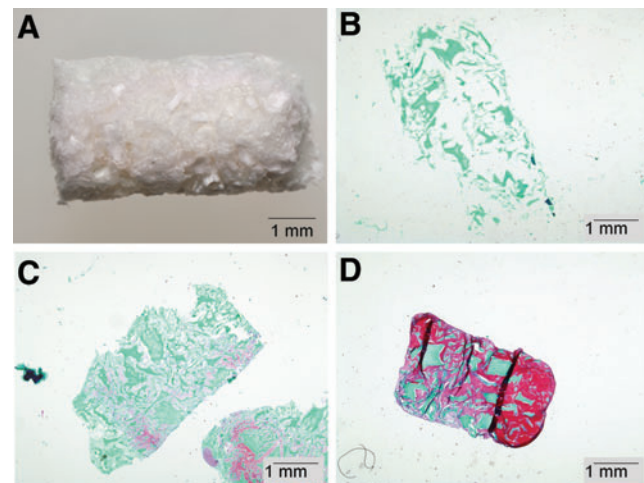


FIG. 1. Extent of MSC chondrogenesis in CDM scaffolds demonstrated by safranin-O staining after 37 days of *in vitro* preconditioning. (B–D) GAGs are stained in red, while the remaining collagenous tissue is stained green. (A) Macroscopic image of unseeded cylindrical CDM scaffold. (B) Safranin-O-stained paraffin section of an unseeded control scaffold, showing no safranin-O-positive components. (C) Safranin-O-stained paraffin section of hMSC-seeded CDM scaffold that was chondrogenically differentiated for 37 days, containing little GAGs. (D) Safranin-O-stained paraffin section of hMSC-seeded CDM scaffold showing extensive GAG deposition by the seeded cells. Note that the cells in (C) and (D) have caused sample compaction as compared with the unseeded scaffold in (B). CDM, cartilage-derived matrix; GAGs, glycosaminoglycans; hMSC, human multipotent stromal cell; MSC, multipotent stromal cells. Color images available online at www.liebertpub.com/tea

version 20. An independent-samples *t*-test was performed, assuming unequal variances, to compare the 2D projected areas containing mineral in images from CDM samples that were MSC seeded (*n* = 14) or unseeded (*n* = 13). A *p* < 0.05 was considered significant.

Results

In vitro chondrogenesis of hMSCs in CDM scaffolds

The hMSCs spread throughout the CDM scaffold pores and formed matrix containing proteoglycans and collagen

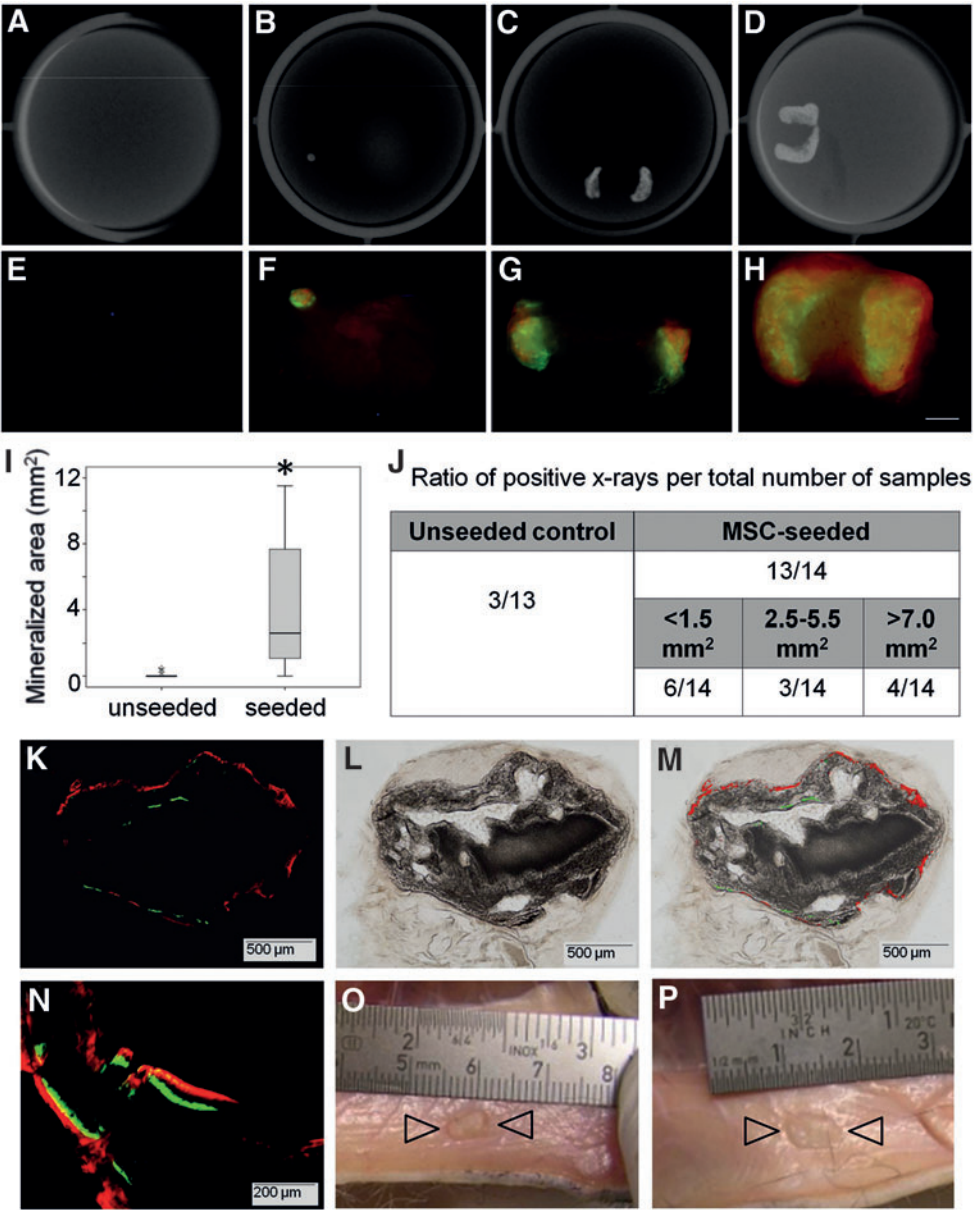


FIG. 2. Significantly more bone was formed in MSC-seeded constructs compared with unseeded CDM. X-ray representations of an average unseeded (A) control sample and the lowest (B), average (C), and highest (D) mineralized areas in MSC-seeded CDM scaffolds, after an 8-week subcutaneous implantation period. (E–H) Whole-mount fluorescence images of the explants (in A–D, respectively) showing the fluorochrome incorporation in the newly formed bone tissue at 3 (red) and 6 (green) weeks of implantation. (I) The extent of mineralization was measured on X-ray images of all explants and calculated as mm² in the 2D representations. Significantly more mineralized tissue formation was observed in the MSC-seeded versus the unseeded samples. Note that the theoretical maximum surface area was 15 mm². **p* < 0.05. (J) The ratio of the numbers of samples showing mineral deposition on X-ray over the total number of samples in that respective group is shown for all samples. For the MSC-seeded samples also, the amount of samples showing lowest (<1.5 mm²), average (2.5–5.5 mm²), and highest (>7.0 mm²) mineralized areas is included. (K–N) In MSC-seeded samples, fluorochrome incorporation was shown on MMA sections. The pattern of fluorochrome incorporation, in general, was that the red (3 week) label was present on the outer periphery of the formed bone, while the green label (6 weeks) was located inward. Macroscopic appearance of MSC-seeded (O) and -unseeded (P) constructs (between arrowheads) on explantation. MMA, methyl methacrylate. Color images available online at www.liebertpub.com/tea

type II, the main cartilage matrix components. Cell differentiation and cell density were inhomogeneous, although hMSCs were seeded according to the same protocol into each scaffold, and the cells were able to spread throughout the complete interior of the CDM scaffolds (Fig. 1). The cells had also invaded several CDM particles. In general, most deposition of glycosaminoglycans (GAGs) was observed at the circular periphery of the constructs.

In vivo ectopic endochondral bone formation in CDM scaffolds

X-ray analysis showed that mineralized tissue was predominantly present in the MSC-seeded samples (Fig. 2). Mineralization in the MSC-seeded constructs was evident by X-ray in 13 out of 14 samples; however, the extent of mineralization varied considerably (Fig. 2B–D). In contrast, negligible mineralization was present in the unseeded CDM scaffolds. The average size of the mineralized area in MSC-seeded constructs was $4.08 \pm 3.75 \text{ mm}^2$, while significantly less mineral deposition ($0.08 \pm 0.17 \text{ mm}^2$, $p=0.002$) was found in the unseeded controls (Fig. 2I). Only three of the unseeded control samples contained a small ($<0.5 \text{ mm}^2$) area that was mineralized under X-ray examination, of which one contained the red fluorochrome. Since the originally implanted cylindrical samples had a 2D-projected surface area of 15 mm^2 , the numbers mentioned earlier would roughly represent $27.2\% \pm 25.0\%$ of mineralized area in the MSC-seeded samples and $0.5\% \pm 1.1\%$ of mineralized area in the unseeded samples.

For the MSC-seeded constructs, it was observed that the red fluorochrome, xylene orange, was incorporated at the

periphery of the newly formed bone tissue at week 3 (Fig. 2L, M). Although calcein green was administered at 3 weeks after xylene orange, it was incorporated inward from the initially delineated area of bone formation at week 6, indicating an inwardly directed progression of mineralization (Fig. 2N).

After 8 weeks of implantation, bone formation was evident in the cell-seeded constructs (Fig. 3). The circular periphery of the 8-week hMSC-seeded constructs harbored cartilaginous tissue containing GAGs and collagen type II (Fig. 3A, B). Both scaffold remnants and tissue deposited by the implanted cells stained positive for collagen type II. Besides, neotissue that was negative for human and equine collagen types I and II was identified at the periphery of the construct as well (indicated by b in Fig. 3B, C). In Figure 3, the development of bone marrow cavities can be observed morphologically, containing both types of marrow: hematopoietic marrow and fatty bone marrow. Furthermore, morphological evidence and the presence of mineralized cartilage further indicated that new bone had formed via the endochondral pathway (Supplementary Fig. S2). However, all samples retrieved after 8 weeks underwent decalcification in Luthra solution, which did not allow staining of collagen types I (rat) and X, TRAP, or von Kossa.

As previously mentioned, one cell-seeded sample was harvested at day 22. Since this sample did not undergo decalcification, it was processed to paraffin to confirm the endochondral process of bone formation. Active matrix remodeling was observed at the circular periphery of this MSC-seeded construct, which indicated endochondral bone formation. At the circular periphery of the implant, tissue

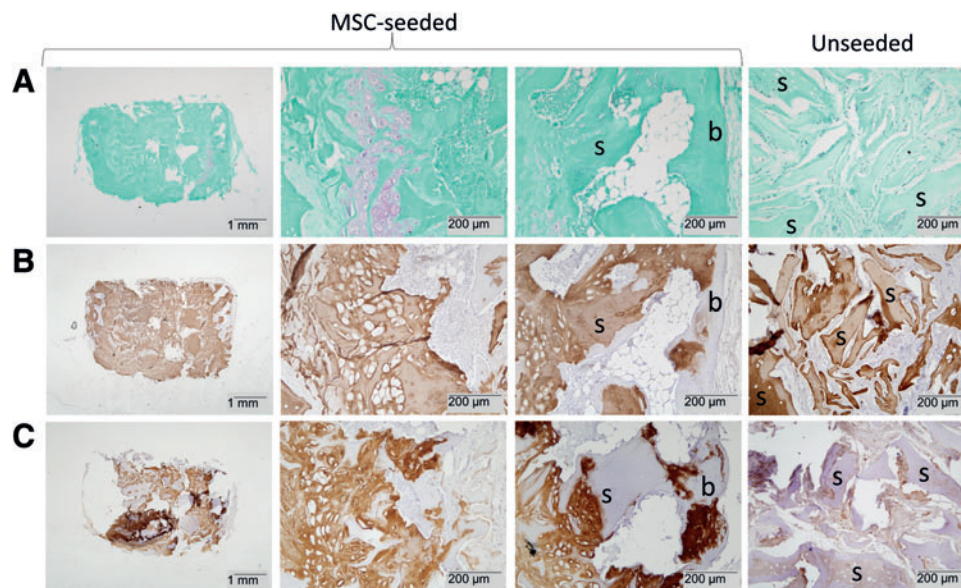


FIG. 3. All aspects of endochondral bone formation were apparent after 8 weeks of subcutaneous implantation in MSC-seeded samples only (columns 1–3). Unseeded samples did not show bone formation (column 4). (A) Cartilaginous neotissue was indicated by safranin-O staining in MSC-seeded constructs. In the lacunae also, hypertrophic cells were present. No safranin-O-stained tissue was observed in the unseeded constructs. (B) At the sites of bone formation, the cartilaginous collagen type II staining is partly replaced by bone (“b” in image, lightly stained in purple by hematoxylin). Unseeded constructs contained collagen type II only in the scaffold material but not in the fibrous ingrowth. (C) Collagen type I of human and/or equine origin was present in the neotissue, between CDM scaffold remnants (s) in MSC-seeded constructs. The scaffold material did not stain for collagen type I. Since the newly formed bone stained negative for human collagen type I, its most likely origin is the rat. Color images available online at www.liebertpub.com/tea

rich in GAGs was present (Fig. 4A). In addition, a matrix rich in collagen type I of human origin was present between the scaffold particles (Fig. 4B). Collagen type II of human and/or equine origin was detected in the newly deposited matrix and in the CDM particles (Fig. 4D). Small areas positive for collagen type X of human origin were observed at the circular periphery of the construct, specifically indicating hypertrophic differentiation of the implanted hMSCs (Fig. 4E). Active remodeling of the hypertrophic cartilage matrix at these sites was shown by a TRAP staining that revealed osteoclast activity (Fig. 4F). The areas undergoing remodeling also contained mineral depositions (Fig. 4G). In addition, the early onset of the formation of bone marrow cavities was observed already after 22 days (Fig. 4C, E). Noteworthy, several small areas of woven bone were visible at the construct periphery, which were not stained by the human and equine collagen antibodies. The patches, however, reacted with a rat-specific antibody for collagen type I, confirming bone formation of rat origin (Fig. 4C).

Finally, the predominant presence of bone formation in the MSC-seeded CDM scaffolds, as compared with the un-

seeded scaffolds, was also observed in the basic fuchsin-stained MMA sections (Fig. 5). The newly formed bone was mainly found at the periphery of the CDM constructs and had a woven and trabecular appearance. At the interface between the CDM matrix and newly formed bone, clear signs of endochondral ossification could be observed with mineralization of the cartilaginous matrix. Within the trabecular bone structure, bone marrow cavities had formed containing both hematopoietic and fatty bone marrow. In contrast to the bone formation in the MSC-seeded scaffold, the resorbed areas of the unseeded scaffolds were replaced by fibrous tissue that also infiltrated the scaffold pores. Only in one construct of the unseeded scaffolds, a very small area of bone formation was observed.

The fate of the implanted human cells was examined by anti-human mitochondrial staining on day 22 and on week 8 after implantation (Supplementary Fig. S3A–D and E–H, respectively). Human cells were detected in the cartilaginous tissue that was deposited by the human cells but not in the fibrous infiltrate. Next to the bone marrow, the tissue's cells were a mixture of human (green arrowhead) and rat

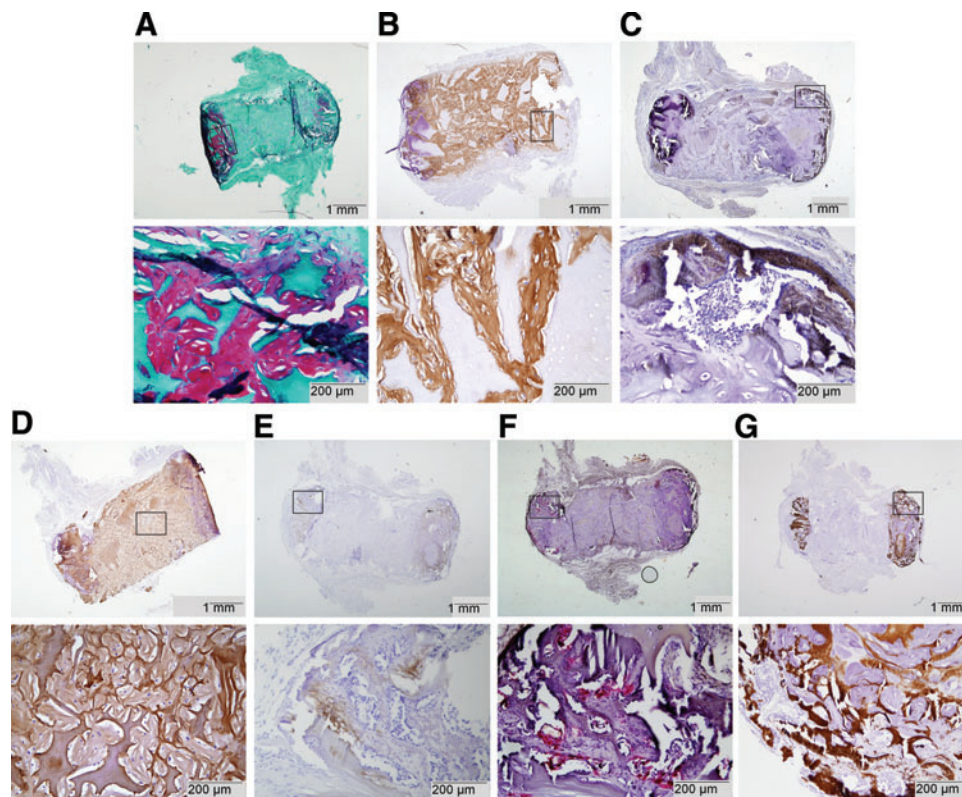


FIG. 4. Tissue formation after 22 days of implantation ($n = 1$) on undecalcified paraffin sections. Active remodeling of cartilaginous matrix into host-derived bone by the endochondral route was shown at the circular ends of the cylindrical construct. *Top* images present the complete cross-section of the constructs and the rectangles illustrate the locations of the corresponding *bottom* images. (A) Safranin-O-stained sections showing the presence of proteoglycans in the construct at the circular cylinder ends. (B) Collagen type I was produced in the constructs by the seeded MSCs. Since the antibody does not detect collagen type I produced by rat cells, it is assumed that this matrix is deposited by the implanted human cells. (C) Collagen type I of rat origin was produced in the construct periphery where the newly formed bone was laid down. (D) Collagen type II was detected both in the equine scaffold material and in the neotissue in the construct. (E) At the circular cylindrical ends, remnants of collagen type X production are shown. This matrix was produced by the implanted cells, as the antibody did not react with rat collagen type X. (F) Active matrix remodeling was revealed by tartrate-resistant acid phosphatase staining of multinucleated osteoclasts in red. (G) Mineralization of predominantly the CDM scaffold was present at the periphery of the construct. Color images available online at www.liebertpub.com/tea

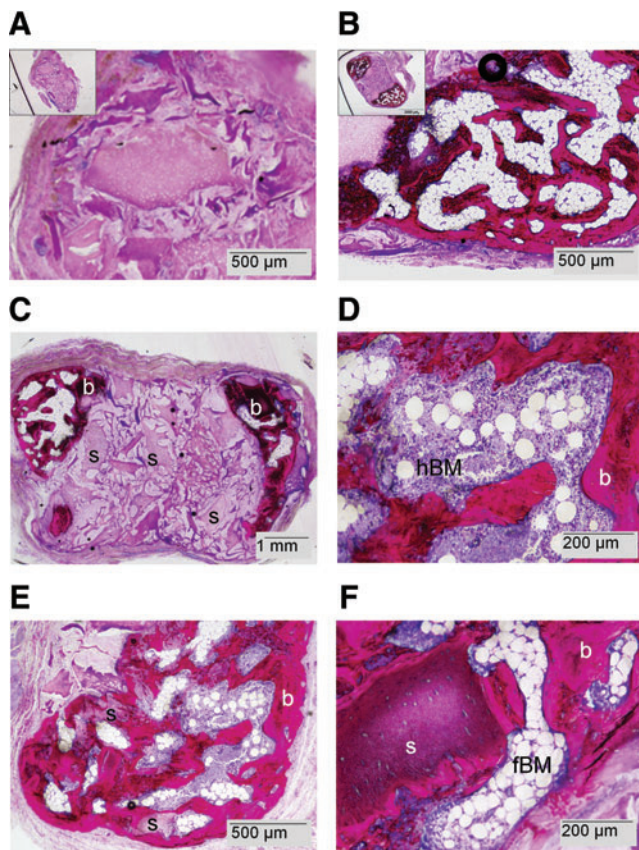


FIG. 5. Bone formation (b) was only present on MMA sections from MSC-seeded constructs after 8 weeks of subcutaneous implantation. *Insets* in (A) and (B) show complete cross sections. Loose fibrous tissue was observed among the CDM particles in unseeded control scaffolds (A), while the seeded samples contained areas of bone formation, including bone marrow cavities (B–F). (C) Bone formation was evident at the construct periphery (B), and scaffold remnants were present (s). The marrow cavities contained hematopoietic bone marrow (D, hBM) and also fatty bone marrow (F, fBM). (E) Besides cell-derived matrix, the CDM particles (s) were also mineralized. Color images available online at www.liebertpub.com/tea

(open arrowhead) cells. On safranin-O-stained consecutive sections, the tissue appeared to be composed of a mixture of newly formed bone (dashed lines) and other tissue. Overall, human cells were present in areas of bone formation but from our results, it was not possible to establish whether they were present in the newly formed bone itself.

Discussion

The concept of developmental engineering¹ suggests that understanding and mimicry of natural processes can assist in improving tissue regeneration. We applied this concept by using current knowledge on endochondral bone development from a cartilaginous tissue template. While most endochondral bone tissue regeneration approaches rely on cartilage tissue engineering to create a cartilage extracellular matrix, we explored the potential of a decellularized cartilaginous scaffold for this purpose. Here, we report on the successful ectopic bone regeneration from a material of xenogenic origin containing xenogenic MSCs and their matrix.

Effects of cells and culture methods

This study showed effective bone regeneration at a subcutaneous location in CDM scaffolds implanted with MSCs. The implanted cells were chondrogenically primed for 37 days before implantation. This preconditioning period did not induce *in vitro* matrix mineralization and was within the previously reported ranges required for induction of ectopic endochondral bone formation from predominantly pellet cultures, varying from two¹ or four², to six¹⁰ or seven⁵ weeks of *in vitro* preconditioning in chondrogenic media. Induction of hypertrophy during the *in vitro* preconditioning period had positive effects,¹ while *in vitro* mineralization of the matrix had negative effects³ on the *in vivo* endochondral process. Overall, the induction of hypertrophy by thyroid hormone was not considered crucial for endochondral bone regeneration^{1,2,5} and, therefore, omitted in this study.

During our preconditioning period, the MSCs had started producing a cartilaginous matrix, rich in GAGs. The most intense staining for GAGs after the *in vitro* preconditioning period was observed at the circular periphery of the constructs. This spatial pattern later coincided with the regions of bone formation in the *in vivo* samples. This tendency may indirectly support the assumption that regions of optimal *in vitro* cartilage tissue formation give rise to *in vivo* bone formation. Moreover, this may explain the variability in the extent of bone formation among the MSC-seeded *in vivo* samples. After all, the applied seeding methods and preconditioning period cannot guarantee homogeneous tissue formation by the MSCs *in vitro* and, thus, no homogeneity in tissue formation on implantation.

In homogeneous tissue differentiation in the constructs could be caused by nutrient limitations.²⁵ However, it is expected that if the geometry of the constructs pores would be carefully controlled, still a considerable increase in construct size can be obtained by adding CDM particles to a construct. In addition, flow perfusion of the *in vitro* culture can also assist in providing sufficient nutrients to the core of the construct.²⁶ The issue of necrotic core development, which can start as soon as the construct is removed from a flow-perfusion system, will, however, still apply to large cartilaginous constructs for endochondral bone formation. Nevertheless, if it would be possible to pinpoint the optimal time window for implantation, dying hypertrophic cells could be implanted that secrete the angiogenic factors. In this way, construct size could be increased without core necrosis.

The timing of events in our study was comparable to those observed during endochondral bone from living cartilage implants,¹³ where the onset was discerned after 3–4 weeks and completion of matrix remodeling into bone by week 8. Further, in line with previous findings,^{2,4} new bone in our CDM scaffolds was formed by host cells that had infiltrated the construct. This was shown by the absence of type I collagen of human origin and abundance of rat-derived collagen type I in the newly formed bone tissue. However, immunohistochemical detection revealed the presence of human cells till 8 weeks after implantation in areas of newly formed bone tissue (Supplementary Fig. S3). It has been previously suggested that implanted MSCs could contribute to bone formation^{2,10} and do not reside in the hematopoietic niche¹⁰ after the hypertrophic cartilage has

been replaced by bone. For transplanted cartilage tissue, it was estimated that 1% of bone cells had originated from the implanted chondrocytes.¹³ In this study, the matrix origin has been identified next to the cellular origin. Our data suggest that overall, new bone consists of rat-specific collagen type I.

The implanted cells were still present at 22 days after implantation, in both cartilaginous and bone-like tissues. It has been reported earlier that these implanted cells actually contribute to the bone formation and end up encapsulated in the bone matrix.^{1,10} The contribution of these cells is still elusive; whether the hypertrophic chondrocytes trans-differentiate to the osteoblastic lineage or the MSCs become osteoblasts directly, or a mixture of both, remains disputable.

Effects of CDM composition

Although equine age is known to affect GAGs in the cartilage matrix,²⁷ this factor is not expected to have a major impact on our results, as our decellularization protocol resulted in negligible amounts of GAG in the CDM scaffolds. In fact, CDM scaffolds contain mainly type II collagen, and collagen composition of equine cartilage has been shown not to significantly change with age.²⁸

The CDM scaffolds that were obtained after decellularization in this study contained negligible remnants of GAGs.²⁹ However, other decellularization protocols may result in as many different scaffold compositions. For example, the GAG content of decellularized cartilage can vary depending on the number of sodium dodecyl sulfate cycles involved.³⁰ Therefore, several decellularized cartilage scaffolds have been developed that contain GAGs,^{30,31} in contrast to the scaffolds evaluated in this study. Notably, in order to retain GAGs in the scaffolds, concessions have to be made in terms of the level of decellularization.¹⁵ Likewise, all other steps in a decellularization protocol can affect the performance of the final product. Future studies may, therefore, focus on elucidation of the influence of CDM composition on *in vivo* bone formation.

The exact contribution of the GAG-rich matrix to ectopic bone formation is unclear. Besides the effects of the seeded cells, the matrix may have been important, as it was lacking in the unseeded control scaffolds. It is, for example, likely that the growth-factor retaining potential of the GAG structures³² played a certain role in, for example, recruitment of host cells and local stimulation of cellular processes. In a previous study, a reduced GAG content of cartilaginous tissues resulted in a delayed progression of bone formation from articular cartilage implants.¹³ In contrast, the removal of GAGs and subsequent inhibition of GAG synthesis did not inhibit bone formation in cartilage that was transplanted to the anterior chamber of the eye.¹³ These contradicting results stress the need for future studies into the necessity of GAGs in decellularized CDM for ectopic endochondral bone regeneration.

Overall, our data indicate that the presence of the MSCs stimulated bone formation. One factor or a combination of the following may have contributed to the onset of endochondral bone formation: component(s) of the decellularized cartilaginous matrix, or the matrix or other factors produced by the MSCs. Future studies may, therefore, incorporate devitalized preconditioned samples to distinguish between the effects of the cells and the matrix or factors they produce.

Further, the simultaneous occurrence of intramembranous bone deposition next to the observed endochondral bone formation cannot be excluded based on our results.

Effects of implantation model

The ectopic implantation model is suitable for screening of the osteoinductive capacity of different construct compositions. Although this environment is challenging for establishing bone formation, MSC-seeded CDM samples successfully regenerated bone tissue. So far, ectopic bone regeneration in devitalized cartilaginous constructs has not been successful.^{12,13,33} Of course, inclusion of healthy, nonimmunocompromised animals in the model could result in a different outcome and will be the subject of our future studies.

This study shows that re-vitalizing a CDM matrix with precultured MSCs in chondrogenic medium helps regain its osteoinductive potential. However, the presence of cells may not be a prerequisite for endochondral bone formation in CDM at orthotopic locations. In previous studies, bone regenerated from unseeded decellularized cartilage in an osteochondral defect in one instance.¹⁵ Since bone marrow-derived MSCs may have access to the scaffold in an osteochondral defect model, an unseeded scaffold will probably behave differently at an orthotopic location or at a site of fracture healing. If, indeed, unseeded scaffolds could stimulate endochondral bone formation at an orthotopic site, there is a great promise for pursuing clinical application by going toward a cell-free, off-the-shelf solution for bone regeneration at orthotopic sites.

Conclusion

Endochondral bone formation at the ectopic location is greatly enhanced by the presence of viable chondrogenic MSCs in decellularized CDM scaffolds compared with unseeded control scaffolds.

Acknowledgments

The authors would like to acknowledge Rick van der Spek, Jason Doppenberg, and Selynda Toma for their input and technical assistance. D.G. was supported by the Dutch Technology Foundation, STW (Veni 11208). K.B. was funded by an Alexandre Suerman Fellowship of the UMC Utrecht. J.M. was supported by the Dutch Arthritis Foundation, and J.V. was supported by the Netherlands Institute for Regenerative Medicine (NIRM).

The antibody against collagen type II (II-II6B3), developed by T.F. Linsenmayer, was obtained from the DSHB developed under the auspices of the NICHD and maintained by The University of Iowa, Department of Biology, Iowa City, IA 52242. The authors are grateful to Dr. E. Muiños Pury Ripalda for providing the protocol for the anti-human mitochondria staining.

Disclosure Statement

No competing financial interests exist.

References

1. Scotti, C., *et al.* Recapitulation of endochondral bone formation using human adult mesenchymal stem cells as a

- paradigm for developmental engineering. *Proc Natl Acad Sci U S A* **107**, 7251, 2010.
2. Farrell, E., *et al.* *In-vivo* generation of bone via endochondral ossification by *in-vitro* chondrogenic priming of adult human and rat mesenchymal stem cells. *BMC Musculoskelet Disord* **12**, 31, 2011.
3. Farrell, E., *et al.* Chondrogenic priming of human bone marrow stromal cells: a better route to bone repair? *Tissue Eng Part C Methods* **15**, 285, 2009.
4. Tortelli, F., *et al.* The development of tissue-engineered bone of different origin through endochondral and intramembranous ossification following the implantation of mesenchymal stem cells and osteoblasts in a murine model. *Biomaterials* **31**, 242, 2010.
5. Pelttari, K., *et al.* Premature induction of hypertrophy during *in vitro* chondrogenesis of human mesenchymal stem cells correlates with calcification and vascular invasion after ectopic transplantation in SCID mice. *Arthritis Rheum* **54**, 3254, 2006.
6. Mackie, E.J., *et al.* Endochondral ossification: how cartilage is converted into bone in the developing skeleton. *Int J Biochem Cell Biol* **40**, 46, 2008.
7. Gawlitta, D., *et al.* Modulating endochondral ossification of multipotent stromal cells for bone regeneration. *Tissue Eng Part B Rev* **16**, 385, 2010.
8. Gawlitta, D., *et al.* Hypoxia impedes hypertrophic chondrogenesis of human multipotent stromal cells. *Tissue Eng Part A* **18**, 1957, 2012.
9. Jukes, J.M., *et al.* Endochondral bone tissue engineering using embryonic stem cells. *Proc Natl Acad Sci U S A* **105**, 6840, 2008.
10. Janicki, P., *et al.* Chondrogenic pre-induction of human mesenchymal stem cells on beta-TCP: enhanced bone quality by endochondral heterotopic bone formation. *Acta Biomater* **6**, 3292, 2010.
11. Gabrielli, M.F., *et al.* Autogenous transplantation of rib cartilage, preserved in glycerol, to the malar process of rats: a histological study. *J Nihon Univ Sch Dent* **28**, 87, 1986.
12. Asch, L., and Asch, G. [Ossification after transplantation of model cartilage in the rat patella]. *Arch Anat Histol Embryol* **72**, 81, 1989.
13. Urist, M.R., and Adams, T. Cartilage or bone induction by articular cartilage. Observations with radioisotope labelling techniques. *J Bone Joint Surg Br* **50**, 198, 1968.
14. Urist, M.R., and Mc, L.F. Osteogenetic potency and new-bone formation by induction in transplants to the anterior chamber of the eye. *J Bone Joint Surg Am* **34-A**, 443, 1952.
15. Benders, K.E., *et al.* Extracellular matrix scaffolds for cartilage and bone regeneration. *Trends Biotechnol* **31**, 169, 2013.
16. Ye, K., *et al.* Bioengineering of articular cartilage: past, present and future. *Regen Med* **8**, 333, 2013.
17. Schwarz, S., *et al.* Processed xenogenic cartilage as innovative biomatrix for cartilage tissue engineering: effects on chondrocyte differentiation and function. *J Tissue Eng Regen Med* 2012 [Epub ahead of print]; DOI: 10.1002/term.1650.
18. Schwarz, S., *et al.* Decellularized cartilage matrix as a novel biomatrix for cartilage tissue-engineering applications. *Tissue Eng Part A* **18**, 2195, 2012.
19. Elder, B.D., Eleswarapu, S.V., and Athanasiou, K.A. Extraction techniques for the decellularization of tissue engineered articular cartilage constructs. *Biomaterials* **30**, 3749, 2009.
20. Malda, J., *et al.* Comparative study of depth-dependent characteristics of equine and human osteochondral tissue from the medial and lateral femoral condyles. *Osteoarthritis Cartilage* **20**, 1147, 2012.
21. Benders, K.E.M., *et al.* Multipotent stromal cells outperform chondrocytes on cartilage-derived matrix scaffolds. *Cartilage* 2014 [Epub ahead of print]; DOI: 10.1177/1947603514535245.
22. Yang, Z., *et al.* Fabrication and repair of cartilage defects with a novel acellular cartilage matrix scaffold. *Tissue Eng Part C Methods* **16**, 865, 2010.
23. van Gaalen, S.M., *et al.* The use of fluorochrome labels for *in vivo* bone tissue engineering research. *Tissue Eng Part B Rev* **16**, 209, 2009.
24. Pautke, C., *et al.* Polychrome labeling of bone with seven different fluorochromes: enhancing fluorochrome discrimination by spectral image analysis. *Bone* **37**, 441, 2005.
25. Malda, J., *et al.* Oxygen gradients in tissue-engineered PEGT/PBT cartilaginous constructs: measurement and modeling. *Biotechnol Bioeng* **86**, 9, 2004.
26. Chen, H.C., and Hu, Y.C. Bioreactors for tissue engineering. *Biotechnol Lett* **28**, 1415, 2006.
27. Platt, D., Bird, J.L., and Bayliss, M.T. Ageing of equine articular cartilage: structure and composition of aggrecan and decorin. *Equine Vet J* **30**, 43, 1998.
28. Brama, P.A., *et al.* Influence of site and age on biochemical characteristics of the collagen network of equine articular cartilage. *Am J Vet Res* **60**, 341, 1999.
29. Benders, K.E.M., *et al.* Multipotent stromal cells outperform chondrocytes on cartilage-derived matrix scaffolds. *Cartilage* **5**, 221, 2014.
30. Kheir, E., *et al.* Development and characterization of an acellular porcine cartilage bone matrix for use in tissue engineering. *J Biomed Mater Res A* **99**, 283, 2011.
31. Yang, Q., *et al.* A cartilage ECM-derived 3-D porous acellular matrix scaffold for *in vivo* cartilage tissue engineering with PKH26-labeled chondrogenic bone marrow-derived mesenchymal stem cells. *Biomaterials* **29**, 2378, 2008.
32. Gandhi, N.S., and Mancera, R.L. The structure of glycosaminoglycans and their interactions with proteins. *Chem Biol Drug Des* **72**, 455, 2008.
33. Barradas, A.M.C., *et al.* *Devitalised Cartilage Matrix as a Template for Bone Formation*. In *TERMIS*, 2010, Galway, Ireland.

Address correspondence to:

Debby Gawlitta, PhD

Department of Orthopaedics, G05.228

University Medical Center Utrecht

P.O. Box 85500

Utrecht 3508 GA

The Netherlands

E-mail: d.gawlitta@umcutrecht.nl

Received: February 19, 2014

Accepted: September 15, 2014

Online Publication Date: November 19, 2014